Biochemical Pharmacology, Vol. 52, pp. 1155–1168, 1996.

ISSN 0006-2952/96/$15.00 + 0.00
PII S0006-2952(96)00424-8

Importance of the Hydrophobic Energy: Structural Determination of a Hypoglycemic Drug of the Meglitinide Family by Nuclear Magnetic Resonance and Molecular Modeling

Laurence Lins,*† *Robert Brasseur*,* *Willy J. Malaisse*,‖
Monique Biesemans,‡ *Patricia Verheyden*‡ *and Rudi Willem*‡

*Numerical Molecular Biophysics Centre, Faculté Universitaire de Gembloux, Gembloux, Belgium; ‖Laboratory of Experimental Medicine, Free University of Brussels (ULB), Brussels, Belgium; ‡High Resolution NMR Centre, Free University of Brussels (VUB), Brussels, Belgium

ABSTRACT. The molecular structure of (2S)-2-benzyl-3-(cis-hexahydro-2-isoindolinylcarbonyl) propionic acid (KAD-1229), a hypoglycemic drug of the meglitinide family, was studied by nuclear magnetic resonance (NMR) and molecular modeling. The results of the NMR experiments indicated that KAD-1229 existed in solution in the form of two stable conformers of equal population, called KADI and KADII in this paper. Three different molecular modelings were then applied: the classical molecular dynamics using the commercial Biosym and Hyperchem softwares and the Prot+ program, which is not based on a dynamical study but on a systematic conformational analysis of the molecule, which includes a term that allows the estimation of the hydrophobic interaction. The modeling results showed the following points. First, in contrast with classical molecular dynamics, which uses restraints from two-dimensional nuclear Overhauser effect (NOE) data, the Prot+ KAD structure provides conformations that support experimental NMR data without any external intervention. In the structures in agreement with NMR data, an important hydrophobic interaction between the phenyl cycle and the perhydroisoindole ring of KAD is observed. This interaction, which seems to play a role in the biological activity of the drug, is lost when no restraints are considered in classical molecular dynamics. Second, the difference between KADI and KADII arises mainly from slight distance geometric differences at the level of the perhydroisoindole and the phenyl rings. BIOCHEM PHARMACOL 52;8:1155–1168, 1996.

KEY WORDS. hydrophobic energy; molecular modeling; hypoglycemic drug; NMR; molecular structure

KAD-1229§ is a new hypoglycemic agent belonging to the meglitinide family [1]. Like hypoglycemic sulfonylureas and other members of the meglitinide family, it apparently owes its insulinotropic action to the closing of ATP-sensitive K^+ channels in pancreatic islet B cells [1–3].

In a recent study using molecular modeling, including a hydrophobic energy term, we underlined the structural analogy between KAD-1229 and other hypoglycemic agents in the meglitinide family and in classical hypoglycemic sulfonylureas [4]. It was proposed that the identification of common molecular determinants responsible for the biological action of these hypoglycemic agents might help in the design of highly active compounds and provide an imprint of their receptor target on the B-cell plasma membrane [4]. These common molecular determinants were essentially a hydrophobic interaction between hydrophobic cycles located at the extremities of each drug molecule; furthermore, we showed that drug activity was related to the distance between both cycles, with activity decreasing with distance [4].

To confirm such an interaction experimentally, we analyzed the KAD-1229 structure by NMR. Three different molecular modelings were then applied: one included a semiempirical equation estimating hydrophobic or solvation energy, and the others used classical energy fields. We show here that the introduction of a solvation energy term in molecular modeling allows the determination of structures in agreement with experimental data in an *ab initio* way, i.e. without giving any other information except the chemical formula of the molecule; the classical dynamics studies, however, only yield *suitable* structures when distance restraints from the NMR experiments are taken into account in the calculations.

† Corresponding author: Dr L. Lins, Numerical Molecular Biophysics Centre, Faculty of Gembloux, Passage des Déportés, 2, B-5030 Gembloux, Belgium. Tel: 32-81 622521/Fax: 32-81 622522.

§ *Abbreviations:* KAD-1229, (2S)-2-benzyl-3-(cis-hexahydro-2-isoindolinylcarbonyl) propionic acid; NMR, nuclear magnetic resonance; CVFF, consistent valence force field; VdW, Van der Waals; ID, one dimensional; 2D, two dimensional; FID, free induction decay.

Received 20 December 1995; accepted 21 May 1996.

MATERIAL AND METHODS

Material

A sample of KAD-1229 was kindly provided by the Kissei Pharmaceutical Company (Matsumoto-City, Japan; patent: EPC 507,534, October 1992).

NMR Experiments

DATA ACQUISITION. The NMR sample was prepared by dissolving ca. 10 mg of KAD-1229 in 100 mL CD_3OD and then adding 400 mL C_6D_6. The sample was subsequently degassed and sealed. All spectra were recorded at 303 K on a Bruker AMX500 spectrometer interfaced with an X32 computer. Chemical shifts were referenced to the residual solvent peak (C_6D_6) and converted to the standard Me_4Si scale by adding 7.15 ppm and 128.0 ppm for ^1H and ^{13}C nuclei, respectively. ^{13}C BB proton decoupled, and DEPT-135 spectra were recorded by using standard pulse sequences and delays.

The proton-detected ^1H–^{13}C correlation spectrum (HMQC-COSY) of the aliphatic part was recorded by using the pulse sequence and phase cycling proposed by Bax *et al.* [5] with ^{13}C decoupling (GARP). Two hundred fifty-six FIDs were recorded and zero-filled to 512 W in the F1 dimension with a spectral width of 5625 Hz. 2K data points, no zero-filling, a spectral width of 1502 Hz (acquisition time 0.68 sec), 16 scans, and a relaxation delay of 1.32 sec were used in the F2 dimension.

A proton-detected heteronuclear multiple bond correlation spectrum (HMBC-COSY) was recorded by using the pulse sequence and phase cycling proposed by Bax and Summers [6]. The experiment was optimized to $^{2,3}J(^1H$–$^{13}C)$ average values of 8.3 Hz (delay = 60 msec). The low-pass J filter was optimized to the $^1J(^1H$–$^{13}C)$ value of 135 Hz. Four hundred FIDs were recorded and zero filled to 1 K in the F1 dimension with a spectral width of 21,625 Hz covering the resonances of the complete ^{13}C spectrum. 2K data points, no zero filling, a spectral width of 3623 Hz (acquisition time, 0.28 sec), 64 scans, and a relaxation delay of 1.72 sec were used in the F2 dimension.

An exclusive correlation spectroscopy (E. COSY) spectrum was recorded with a spectral width of 1805 Hz by using the pulse sequence and phase cycling proposed by Griesinger *et al.* [7]. In the F1 dimension, 256 FIDs zero filled to

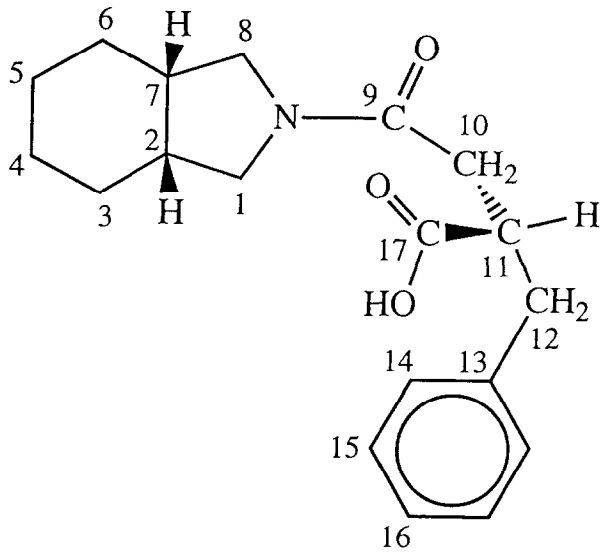

FIG. 1. Structure of KAD-1229.

TABLE 1. ^1H and ^{13}C chemical shift data (in ppm) of the two conformations KADI and KADII of KAD-1229

	^{13}C			^1H	
		KADI		KADII	
		a	b	a	b
1	49.85	3.303 (−11.2, 5.5)	3.255 (−11.2, 7.0)	3.333 (−12.0, 6.8)	3.247 (−12.0, 5.5)
2	35.93, 35.99	1.747		1.758	
3*	25.46	1.33	1.17	1.30	1.17
4,5	22.62, 22.84	strongly overlapping resonances between 1.10 and 1.35			
6*	25.71	1.22	1.06	1.30	1.06
7	37.43	1.787		1.757	
8	50.20, 50.29	2.993 (−10.0, 7.0)	2.739 (−10.0, 6.2)	2.931 (−10.0, 6.0)	2.747 (−10.0, 7.0)
9	171.3				
10	35.17	2.609 (−16.2, 9.0)	2.254 (−16.2, 4.3)	2.586 (−16.2, 9.2)	2.182 (−16.2, 4.5)
11	43.31, 43.38	3.475		3.465	
12	37.95, 38.01	3.251 (−13.7, 5.7)	2.951 (−13.7, 8.6)	3.261 (−13.7, 5.7)	2.907 (−13.7, 8.6)
13	139.3, 139.4				
14	129.4	7.25		7.25	
15	128.8	7.25		7.25	
16	126.8	7.15		7.15	
17	177.4				

^{13}C chemical shifts were obtained from a proton-decoupled spectrum. ^1H shifts were obtained from ID-proton and/or proton-detected ^1H–^{13}C HMQC-COSY spectra. The values between parentheses are $^2J(^1H$–$^1H)$ and $^3J(^1H$–$^1H)$ coupling constants (in Hz), respectively.

* Assignment interchangeable pairwise. The assignments of 1 and 8 were made arbitrarily; consequently if this assignment has to be interchanged, 2 and 7 and 3 and 6 will also have to be interchanged.

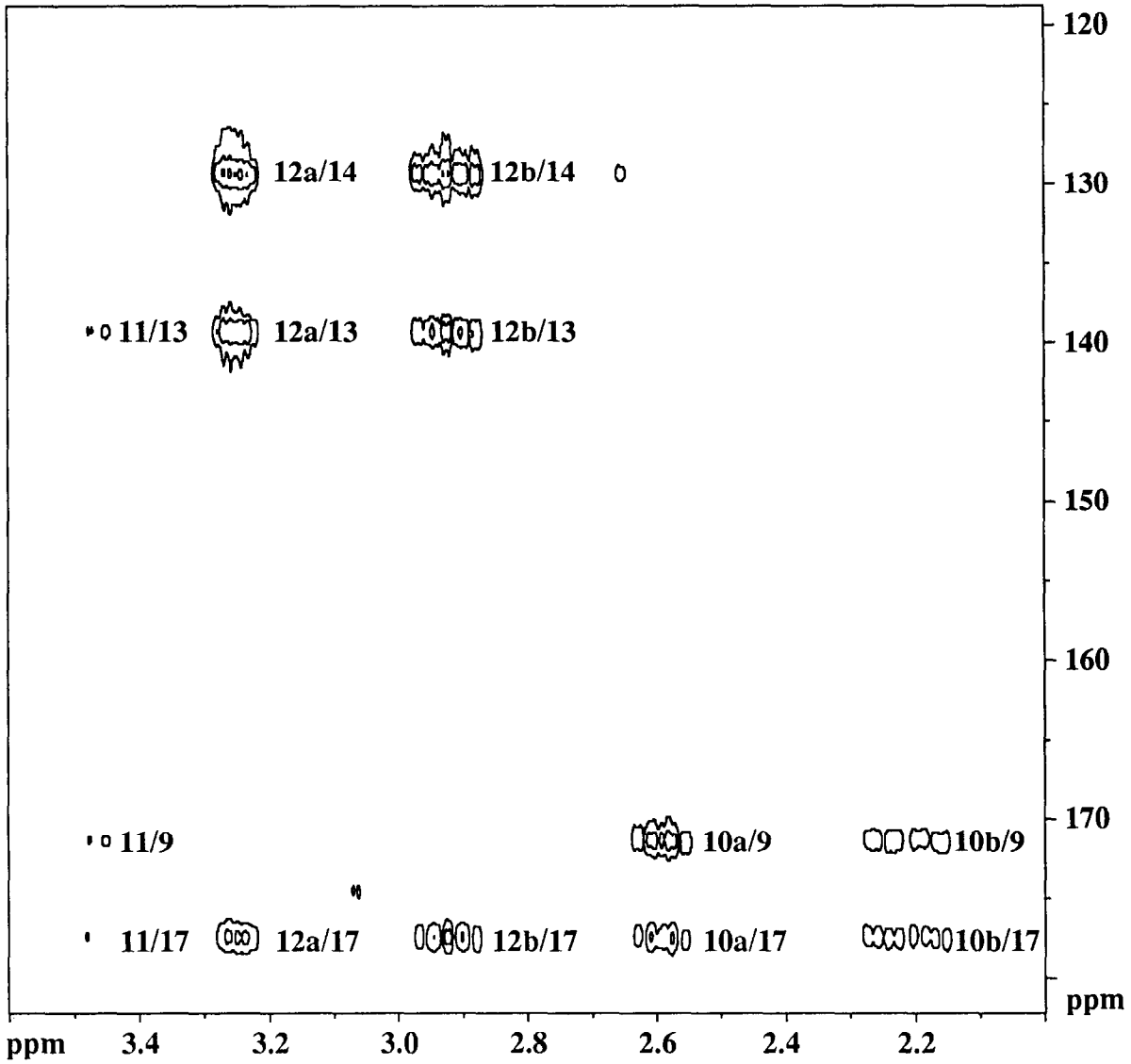

FIG. 2. F1 low-field expansion of the HMBC-COSY spectrum. F1 axis (vertical) ^{13}C chemical shifts; F2 axis (horizontal) proton chemical shifts. Some important cross peaks are indicated.

2 K were used; 4K data points, no zero filling (acquisition time, 1.13 sec), 36 scans, and a relaxation delay of 1.37 sec were used in the F2 dimension.

Ten 2D NOESY [8] spectra were recorded by using TPPI [9] with a spectral width of 3759 Hz; 256 FIDs were recorded and zero filled to 1 K in the F1 dimension; 2K data points, no zero filling, (acquisition time, 0.27 sec), 32 scans, and a relaxation delay of 1.73 sec were used in the F2 dimension. The mixing times had values from 200 to 1100 msec in steps of 100 msec.

PROTON–PROTON DISTANCES FROM 2D NOESY BUILD-UP EXPERIMENTS. Proton–proton distances were determined from the formula $r_{kl} = r_{ref} (S_{ref}/S_{kl})^{1/6}$ [10] where r_{kl} represents the distance of interest between the protons k and l; r_{ref} represents the reference distance separating two protons, the mutual distance of which is unambiguously established from geometrical considerations; S_{kl} is the slope of the build-up straight line, as defined below, in the initial rate approximation, associated with the cross peaks correlating the pairs of protons k and l; and these build-up straight lines represent the growth of the cross peak V_{kl}, normalized to the autopeak V_{ll} of the same F2 coordinate, as a function of the mixing time. When the integration of the autopeak is impossible because of resonance overlap, normalization is performed to the average value of autopeak volumes of protons with similar T_1 relaxation characteristics [11]. S_{ref} is the corresponding slope associated with the reference pair of protons.

The reference distance r_{ref} is the distance of 1.76 Å separating the two hydrogen atoms of a methylene group, as calculated from standard C–H bond lengths and H–C–H bond angles of tetrahedral carbon atoms. The pair of reference protons chosen was that of methylene group 10 because the two cross peaks associated with this pair exhibited

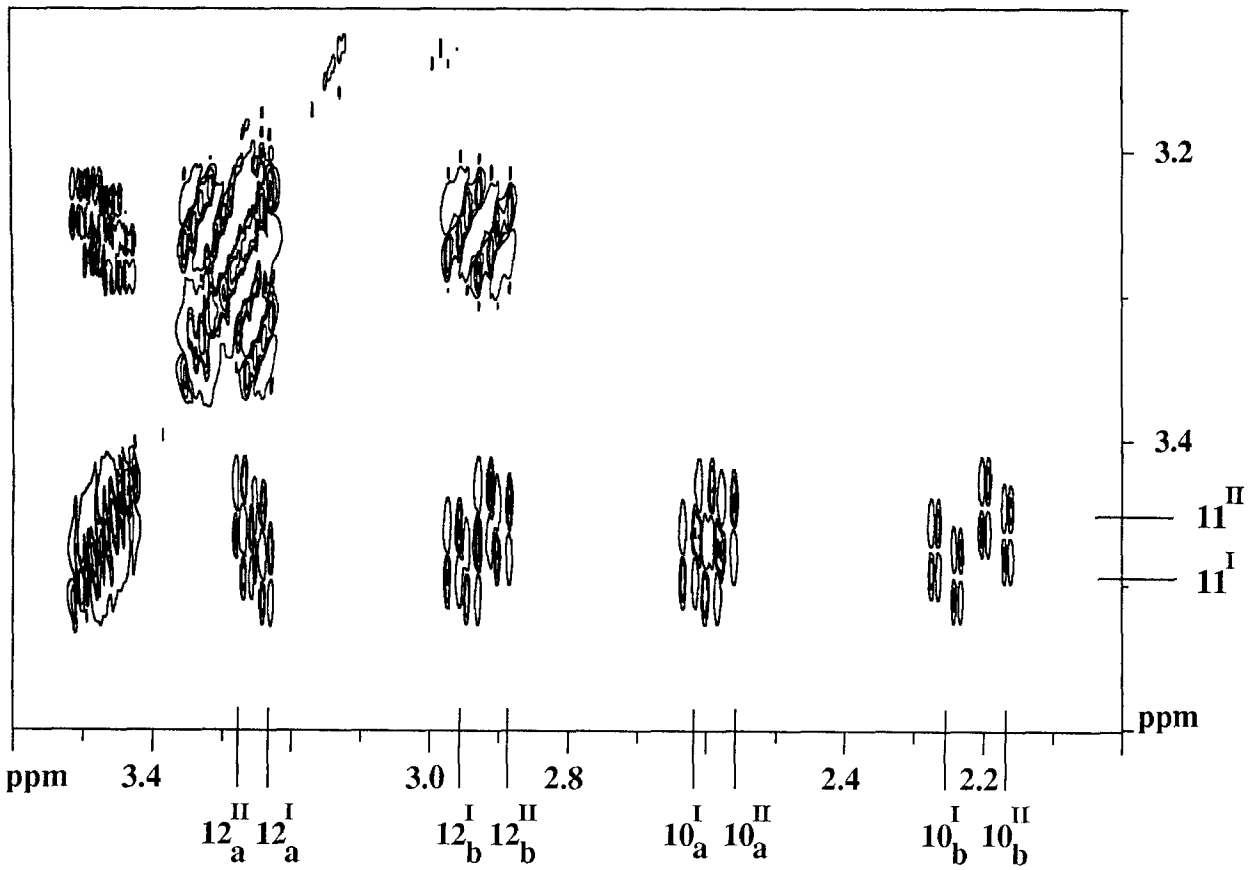

FIG. 3. Expansion of the 2D E.COSY spectrum. F1 and F2 axes are proton chemical shift scales. Note the clear discrimination between the two conformations for the resonances of protons 11 in the F1 dimension and protons 10 and 12 in the F2 dimension.

identical build-up slopes to within 2% as determined from straight lines displaying correlation coefficients >0.995 with 10 build-up points and because they display the least overlap with other protons.

When the slopes associated with a pair of cross peaks arising from the interacting protons *k* and *l* differed by less than 20%, the mean value was used to calculate the distance. When the slopes differed by more than 20%, the one resulting from the least overlapping peaks and/or displaying the highest correlation coefficient was selected.

Molecular Modeling

METHOD 1 (BIOSYM SOFTWARE). Molecular dynamics simulations were performed on a Silicon Graphics Indigo 2 by using the Insight and Discover (version 2.9.5) software from Biosym (Insight II User Guide, version 2.3.0, Biosym Technologies, San Diego, CA, USA). The CVFF potential function was used. The calculated NOE distances were decreased and increased by 10% to give 18 lower and 18 upper limit restraints for the first conformer, KADI, and 17 upper and 17 lower for the second conformer, KADII. Because of the overlap of the 8b protons of KADI and KADII, the NOE between 8b and 14 (Fig. 1) cannot be attributed unambiguously. Because this NOE may be the result of a short distance in either KADI or KADII or in both, two restrained molecular dynamics runs were performed for both KADI and KADII, one including this restraint and one without.

A restrained molecular dynamics run using distance restraints was comprised of 250 psec dynamics at 900 K, saving the structure every 5 psec. The resulting 50 structures were cooled down to 300 K, followed by 10 psec dynamics, and were then energy minimized using steepest descents and conjugate gradient minimization, resulting in 50 low-energy structures.

METHOD 2 (HYPERCHEM SOFTWARE). Molecular dynamics was also performed with the Hyperchem software, version 4.0, on a Pentium processor microcomputer. The MM+ force field, derived from the MM2 force field described by Allinger [12], was used. This force field is recommended particularly for structure simulations on small organic compounds. The proton–proton distances from the NMR spectra unambiguously assigned to KADI and KADII were also used as restraints, together with the 8b/14 distance (Fig. 1). The molecular dynamics was performed under conditions similar to those in method 1, i.e. in vacuo at a temperature of 900 K with a heat time of 10 psec, a run time of 250 psec, and a cool time of 10 psec (the structure

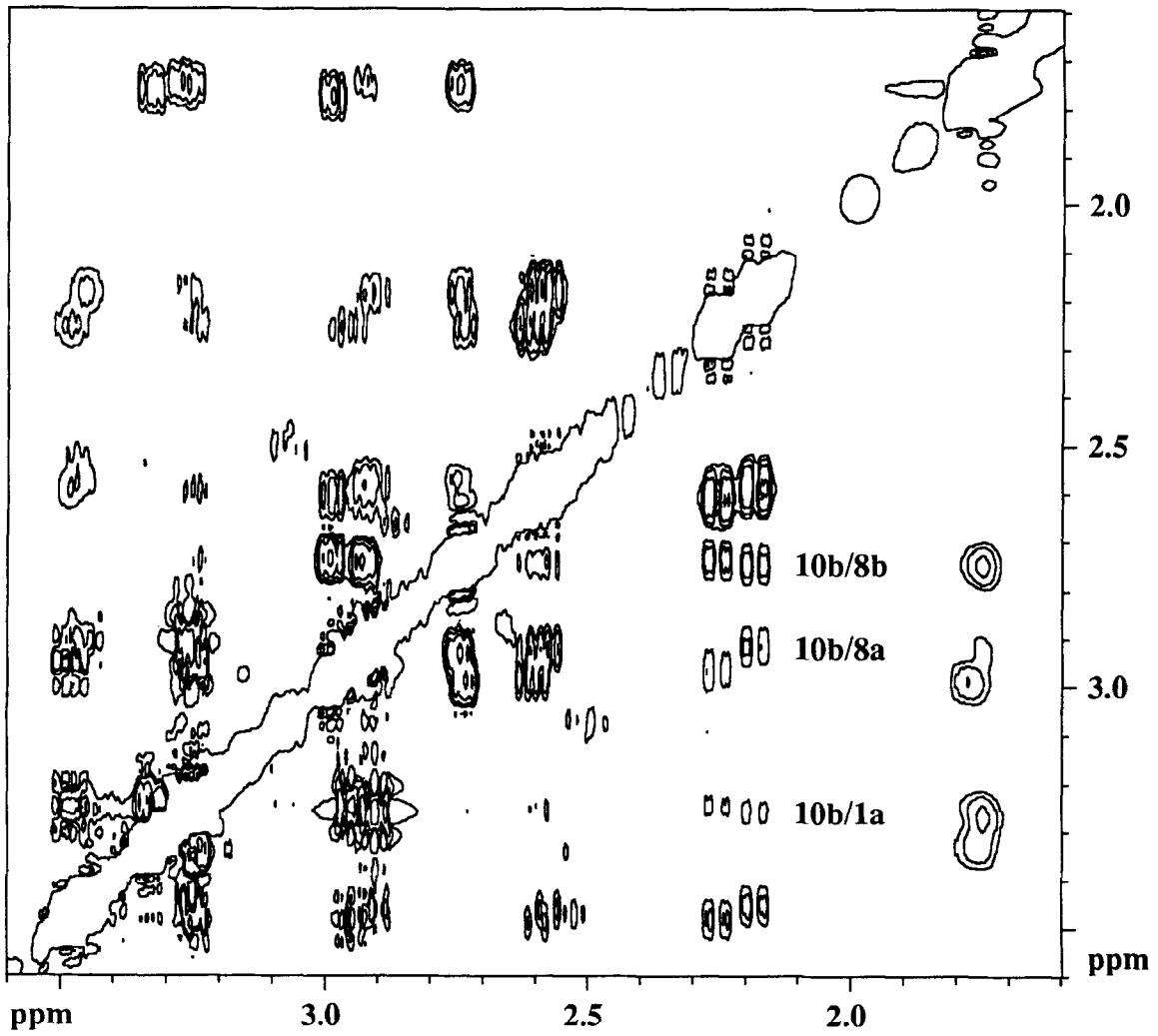

FIG. 4. Expansion of a 2D NOESY spectrum. F1 and F2 axes are proton chemical shift scales. The crucial cross peaks correlating the two networks of mutually coupled spin systems are outlined.

is cooled down to 300 K). The step size was 5.10^{-4} psec. The resulting structure was then energy minimized by using a Polak-Ribiere conjugate gradient.

METHOD 3 (PC-PROT + SOFTWARE). The conformational analysis of KADI and KADII is based on a semiempirical procedure [13]. In this approach, total conformational analysis is calculated as the sum of all the contributions due to the VdW energy, torsional potential, electrostatic interactions [13], and hydrophobic interactions [14]. The latter are taken into account through the calculation of solvation energy based on an empirical equation [14]. This equation describes the free energy of solvation between atoms i and j:

$$Etr_{ij} = \delta_{ij} (|E_{tri} f_{ij}| + |E_{trj} f_{ji}|) \exp((r_i + r_j - d_{ij})/2r_{sol}) \quad [1]$$

where δ_{ij} is -1 when atoms i and j are either both hydrophobic or both hydrophilic and $+1$ otherwise; E_{tri} and E_{trj} are the free energies of transfer from a hydrophobic to a hydrophilic phase; r_i and r_j are the radii of atoms i and j, respectively; d_{ij} is the distance between atomic centers; and r_{sol} is the radius of a solvent molecule. The parameter f_{ij} represents the portion of atom i covered by atom j and is calculated as follows [14, 15]:

$$f_{ij} = \frac{C_j}{S_{ij}}\left(1 - \frac{d_{ij} - r_i - r_j}{2r_{sol}}\right) = \frac{r_j^2}{4(r_i + r_j)^2}\left(1 - \frac{d_{ij} - r_i - r_j}{2r_{sol}}\right)$$

where C_j is the surface of a circle of radius r_j and S_{ij} the surface of a sphere of radius $r_i + r_j$. In a condensed medium, the fractional area of atom i covered by its neighbors is 1. The fractional area of i covered by j is f_{ij}, such that $0 < f_{ij} < 1$. This parameter decreases to zero when the distance between i and j is large enough to accommodate a solvent molecule between them. The surface of an atom i covered by other atoms of the same molecule is summed up, and an estimation of the solvent accessible surface is obtained by subtracting that sum from the entire surface of i.

The total interaction energy between atoms i and j is equal to the sum of the VdW energy, electrostatic energy,

TABLE 2. Proton–proton distances in solution as obtained from 2D NOESY NMR data

	Distance (Å)		
Proton pairs	**KADI**	**KADII**	**KADI or KADII***
1a/1b	1.87		
1a/2		2.24	
1a/3a	2.47		
1a/3b	2.42		
1b/3a		2.42	
1b/3b		2.56	
1a/10a		3.26†	
1b/10a	3.14†		
1b/10b	3.06	3.08	
6a/7	2.41		
6b/7	2.58		
6a/8a		2.50	
6a/8b	2.57		
6b/8a	3.52†	2.54	
6b/8b	2.65	2.79	
7/8a	2.25	3.38‡	
8a/8b	1.85	1.82	
8a/10a	2.37	2.20	
8b/10b	2.47	2.49	
8b/14			4.08†
10a/10b	1.76 (ref)	1.76 (ref)	
10b/11	2.62	2.56	
10b/12b	2.80	2.78	
10b/14	3.16‡	3.37	

* Distances not unequivocally assigned to either KADI or KADII.
† Values obtained from correlations <0.95.
‡ Values obtained from only one cross peak.

torsional potential, and the mutual solvation energy of atoms *i* and *j* and that of the solvent. The free energy of solvation consists of two elements: the interaction energy between solute and solvent molecules and that between the atoms of the solute molecule. Actually, any atom interacting with another atom does not distinguish whether this atom belongs to the solute or to the solvent molecule. Each atom will tend to interact with another having the same hydrophobic/hydrophilic properties, independently of the concept of solute or solvent.

The conformation of the molecules is first analyzed by a systematic analysis structure tree applied on each torsional angle. The lowest conformational energy of the most probable structure resulting from this step is subsequently obtained by energy minimization by using the Simplex method [16].

The values used for the valence angles, bond lengths, atomic charges, torsional potential, and energy values for the VdW interactions are those used in Method 2 (Hyperchem software) because the molecules were built using this program. The force field used in Hyperchem is the MM+ force field [12]. The resulting structure is then reintroduced into the PC-PROT+ program for systematic and energy minimization steps.

Calculations were performed on a Pentium processor microcomputer with the PC-PROT+ (Protein Analysis Programs) procedure. Graphs were drawn with the PC-MGM+ (Molecular Graphics Manipulation) and the WinMGM [17] programs.

CALCULATION OF RELATIVE POPULATION OF KADI AND KADII. The relative conformational probability of both conformers was calculated with the following equations:

$$P_I = \frac{e^{-E_I/kT}}{e^{-E_I/kT} + e^{-E_{II}/kT}}$$

and

$$P_{II} = \frac{e^{-E_{II}/kT}}{e^{-E_I/kT} + e^{-E_{II}/kT}}$$

with T = 298 K and E_I and E_{II} corresponding to the internal energy of the KADI and KADII conformers, respectively [18].

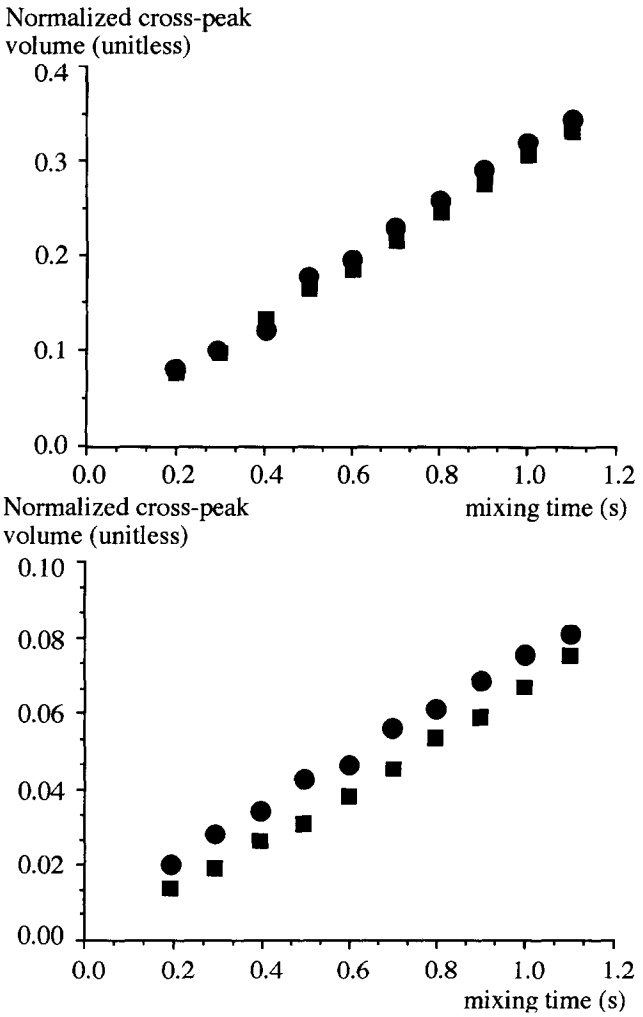

FIG. 5. Two examples of 2D NOESY build-up curves. (Top) For the cross peak arising from the H atoms, H(10a) and H(10b) were used as reference for the determination of the solution-state distances. (Bottom) A typical cross peak pair without resonance overlapping from the H atoms H (7a) and H (8).

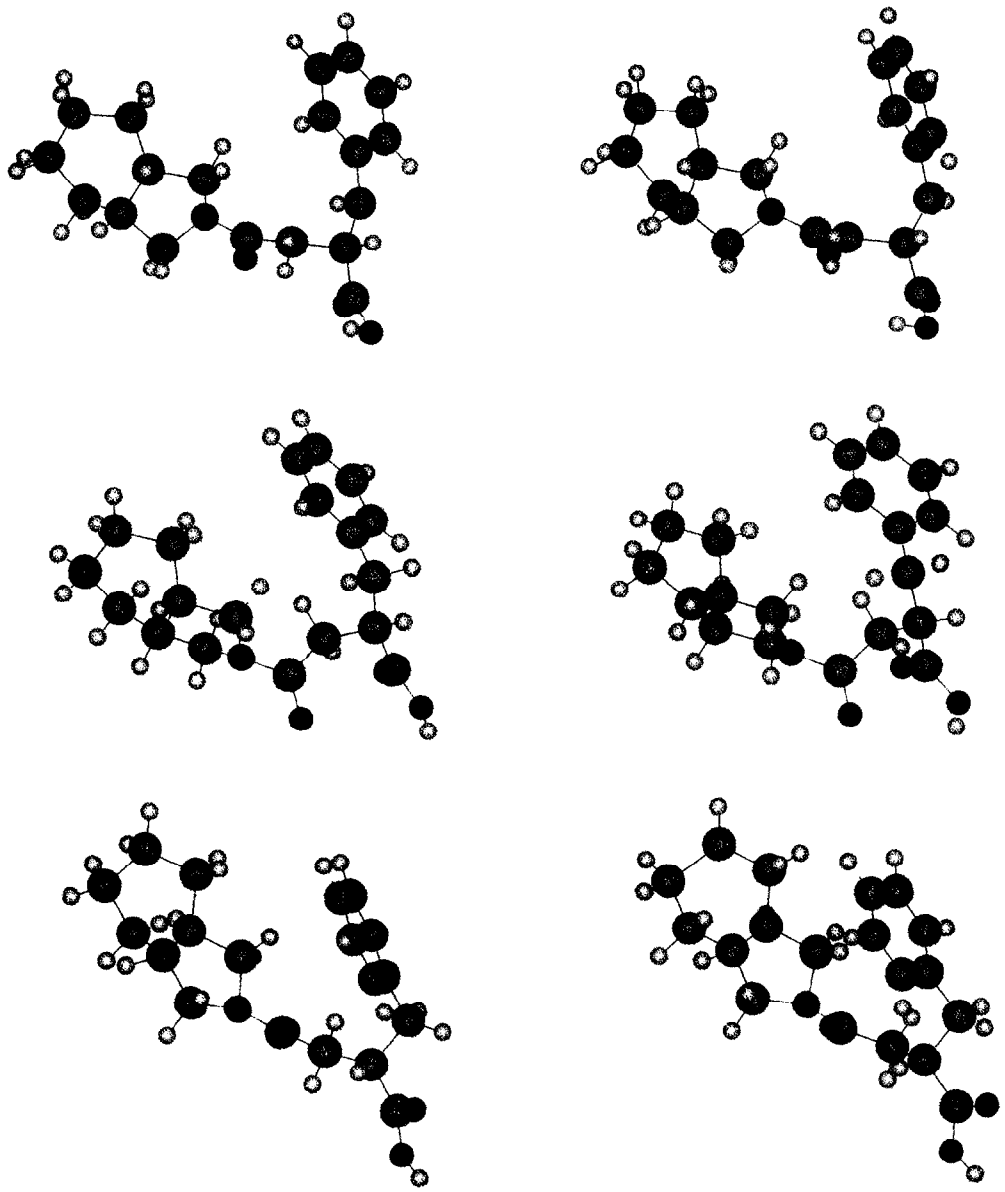

FIG. 6. Stereoview of the KADI structure represented in balls obtained by Method 1 (upper panel) and Method 2 (middle panel) using distance restraints, and by Method 3 (lower panel) including hydrophobic interactions. Large dark gray and small light gray balls represent carbon and hydrogen atoms, respectively; blue and red balls are nitrogen and oxygen atoms, respectively.

RESULTS AND DISCUSSION

NMR Studies of the Solution Structure

^{1}H AND ^{13}C RESONANCE ASSIGNMENT. The 1D ^{1}H and ^{13}C spectra of KAD-1229 (Fig. 1) in a mixture of CD_3OD/C_6D_6 (1/4) revealed an unexpected and puzzling splitting of a series of signals into pairs of resonances with approximately equal intensities.

To rule out the formation of a nonsymmetrical dimer, we recorded these 1D spectra in several other solvents, such as $CDCl_3$, acetone-d6, and CD_3OD. A comparable splitting was observed in all cases. We consequently attributed the splitting of the resonances to the presence of two stable conformations of similar energy. An attempt to observe a possible coalescence of such pairs of resonances by heating up a toluene-d6 solution of the sample resulted in the irreversible appearance of numerous additional resonances resulting from the decomposition of KAD 1229. The final ^{1}H and ^{13}C assignments are presented in Table 1.

In the perhydroisoindole ring, the carbon resonances at 49.85 ppm and the pair at 50.20 and 50.29 ppm, being compatible with resonances of carbon atoms next to nitrogen, were assigned arbitrarily to carbon atoms 1 and 8, respectively. From this starting point, the chemical shifts of the corresponding hydrogen atoms were obvious from the HMQC-COSY spectrum [5] exhibiting $^1J(^1H–^{13}C)$ correlations. However, the complete carbon and proton network

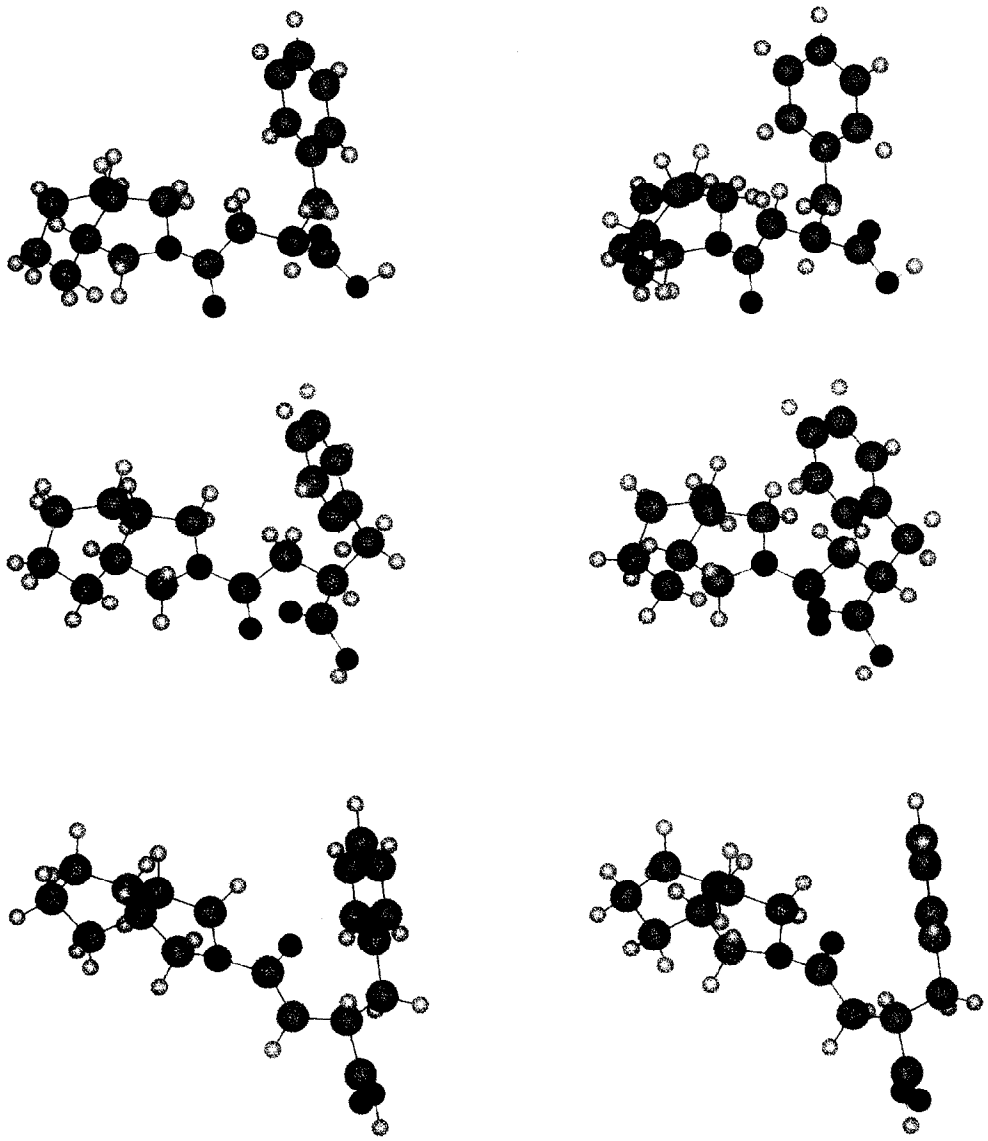

FIG. 7. Stereoview of the KADII structure represented in balls obtained by Method 1 (upper panel) and Method 2 (middle panel) using distance restraints and with Method 3 (lower panel). Same representation as in Fig. 6.

in the perhydroisoindole ring, with no complete conformation specific assignment, could be unraveled further by the $^{2,3}J(^{1}H-^{13}C)$ correlations exhibited in the HMBC-COSY spectrum [6]. From the amide carbon resonance at 171.3 ppm and the carboxylic acid carbon resonance at 177.4 ppm, protons 10–12 and thus the corresponding carbon resonances could be assigned (Fig. 2). The resonance assignment was completed with the aromatic carbon and proton atoms.

Because the chemical shift difference between corresponding ^{13}C resonances of the two conformations is very small, no further attempt to discriminate the two conformations could reasonably be undertaken at this stage. However, the proton resonances could be assigned further. Thus, careful analysis of the E.COSY spectrum [7], a $^{1}H-^{1}H$ correlation technique that exhibits a simplified multiplet pattern compared with the classical DQF-COSY (Fig. 3), made possible an almost complete assignment of the two coupled proton systems, the perhydroisoindole ring and the "amide" chain, together with the corresponding coupling constants, where possible.

Because these two systems are separated by an amide bond, no connection between these parts of the molecule could be made at this point. Analysis of the 2D NOESY spectrum [8, 10] (Fig. 4) finally completed the assignment because cross peaks resulting from intramolecular dipolar cross relaxation [8] through space were found between protons 1 and 10 and 8 and 10, so that connection between the two coupled spin networks of the molecule was eventually achieved.

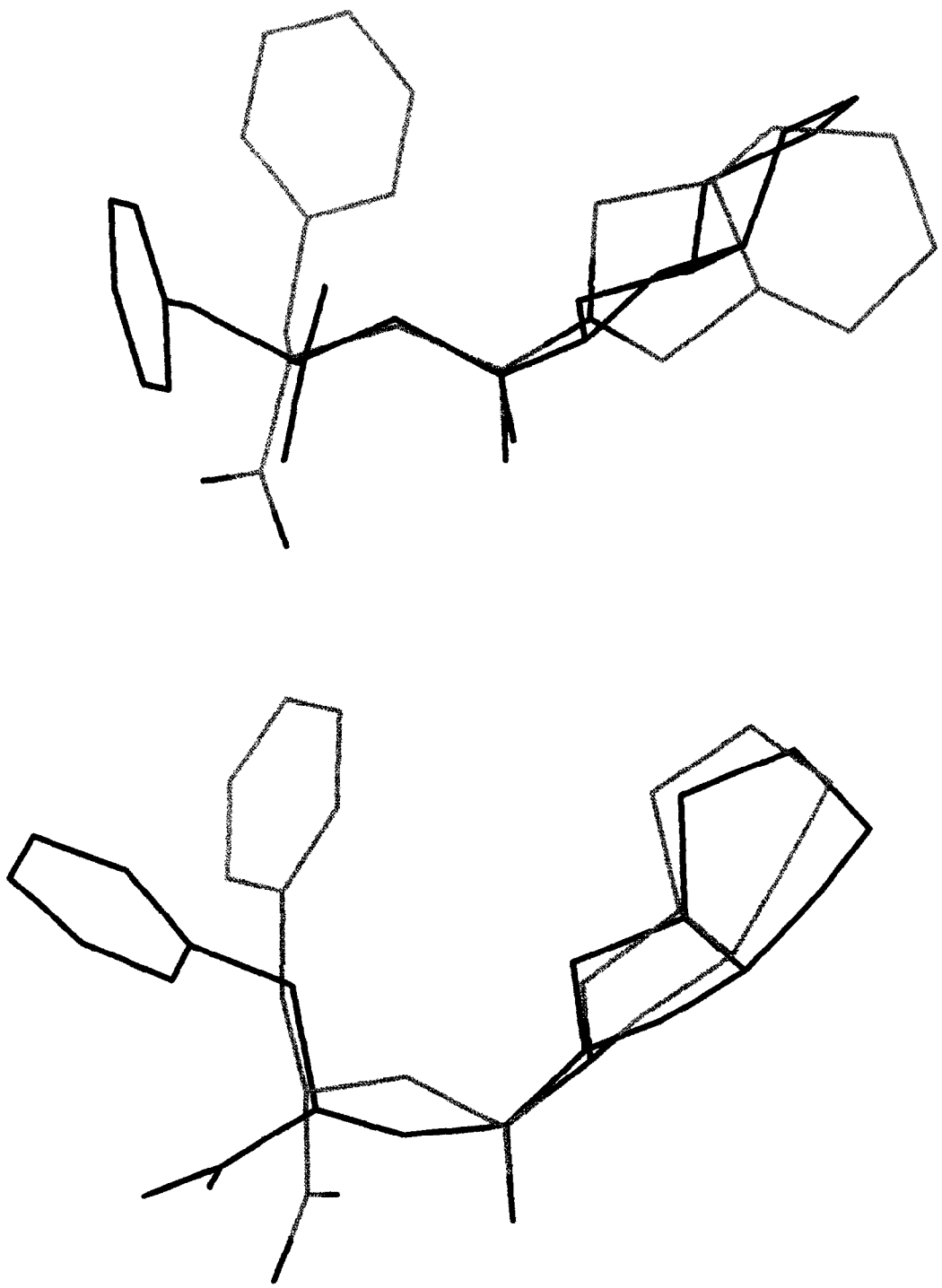

FIG. 8. Superposition of the KADI structure obtained with all distance restraints (colors as defined in Fig. 6) and without the 8b–14 distance restraint for Method 1, or no distance restraints for Method 2 (in green) using Method 1 (upper panel) and Method 2 (lower panel).

PROTON–PROTON DISTANCES IN SOLUTION. The proton–proton distances that could be determined from the 2D NOESY build-up experiment in the initial rate approximation are reviewed in Table 2 [8, 10, 11].

Two examples of build-up straight lines from which these distances are determined are displayed in Fig. 5. All the build-up curves were obtained from negative cross peaks, being of opposite sign with respect to the positive autopeaks, indicating conditions of extreme narrowing [10]. In view of the restrained molecular modeling calculations per-

TABLE 3. Comparison between NMR proton–proton distances of KADI and KADII and distances measured on the modeled structures obtained by Method 1 (Biosym), Method 2 (Hyperchem), and Method 3 (Prot+)

Proton pairs	NMR distance (Å)	Method 1 without restraints on 8b/14	Method 1 with restraints on 8b/14	Method 2 without any restraint	Method 2 with all restraints	Method 3
A: KADI						
1a/1b	1.87	1.92	1.80	1.79	1.77	1.78
1a/3a	2.47	2.82	2.73	2.47	2.23	2.34
1a/3b	2.42	2.69	2.65	3.34	3.24	2.71
1b/10a	3.14	3.55	4.02	5.09	3.13	4.61
1b/10b	3.06	4.51	3.55	4.78	3.52	4.78
6a/7	2.41	2.36	2.35	2.47	2.47	2.10
6b/7	2.58	2.57	3.00	3.06	3.03	2.75
6a/8b	2.57	2.71	2.86	2.46	2.48	2.71
6b/8a	3.52	3.08	3.60	2.81	3.40	3.43
6b/8b	2.65	2.71	2.36	3.06	3.71	2.84
7/8a	2.25	2.19	2.26	3.04	2.91	2.88
8a/8b	1.85	1.85	1.77	1.80	1.75	1.78
8a/10a	2.37	2.38	2.78	4.15	3.80	4.24
8b/10b	2.47	2.67	2.32	2.34	2.19	2.86
8b/14	4.08	5.70	3.26	5.73	3.75	3.57
10a/10b	1.76	1.77	1.72	1.75	1.77	1.87
10b/11	2.62	2.56	2.37	3.17	2.72	2.98
10b/12b	2.80	3.13	3.20	2.89	2.82	2.28
10b/14	3.16	2.71	3.52	4.90	3.46	2.72
B: KADII						
1a/2	2.24	2.35	2.35	2.32		
1b/3a	2.42	2.78	2.58	2.42		
1b/3b	2.56	2.78	2.68	2.43		
1a/10a	3.26	3.72	4.51	4.14		
1b/10b	3.08	3.79	3.92	4.44		
6a/8a	2.50	2.40	2.43	2.43		
6b/8a	2.54	2.78	2.78	2.43		
6b/8b	2.79	3.31	3.27	3.22		
7/8a	3.38	2.93	2.99	2.68		
8a/8b	1.85	1.78	1.76	1.78		
8a/10a	2.20	2.58	2.58	4.37		
8b/10b	2.49	2.75	2.20	3.92		
8b/14	4.08	4.83	3.97	3.94		
10a/10b	1.76	1.73	1.75	1.78		
10b/11	2.56	2.59	3.06	2.99		
10b/12b	2.81	2.83	3.19	2.22		
10b/14	3.37	3.31	3.11	2.85		

formed with these distances (see below), the long range correlation, observed between the 8b and the aromatic 14 protons, is of extreme importance. Unfortunately, the chemical shift difference between the 8b protons of the two conformations was too small to make an unequivocal assignment. Attempts to enlarge the chemical shift difference by recording the spectra at different temperatures remained unsuccessful.

Molecular Modeling

To fit data to a molecular structure for KAD-1229, three different approaches were used: classical restrained molecular dynamics using Method 1 (Biosym software), with or without the restraint between protons 8b and 14 (to check the importance of this proton–proton distance) and Method 2 (Hyperchem software), with restraints on all proton–proton distances from Table 2, or without any restraints (to compare the classical dynamics studies with Method 3, which operates without any restraint, see below). An *ab initio* method (Method 3: PC-PROT+ software) based on a semiempirical procedure described previously [13] was also used. Briefly, the latter consists of a systematic study of each torsional angle of the molecule followed by a Simplex energy minimization procedure [16]. This approach does not involve restraints, but the energy fields include a term that estimates the hydrophobic interaction [14, 15].

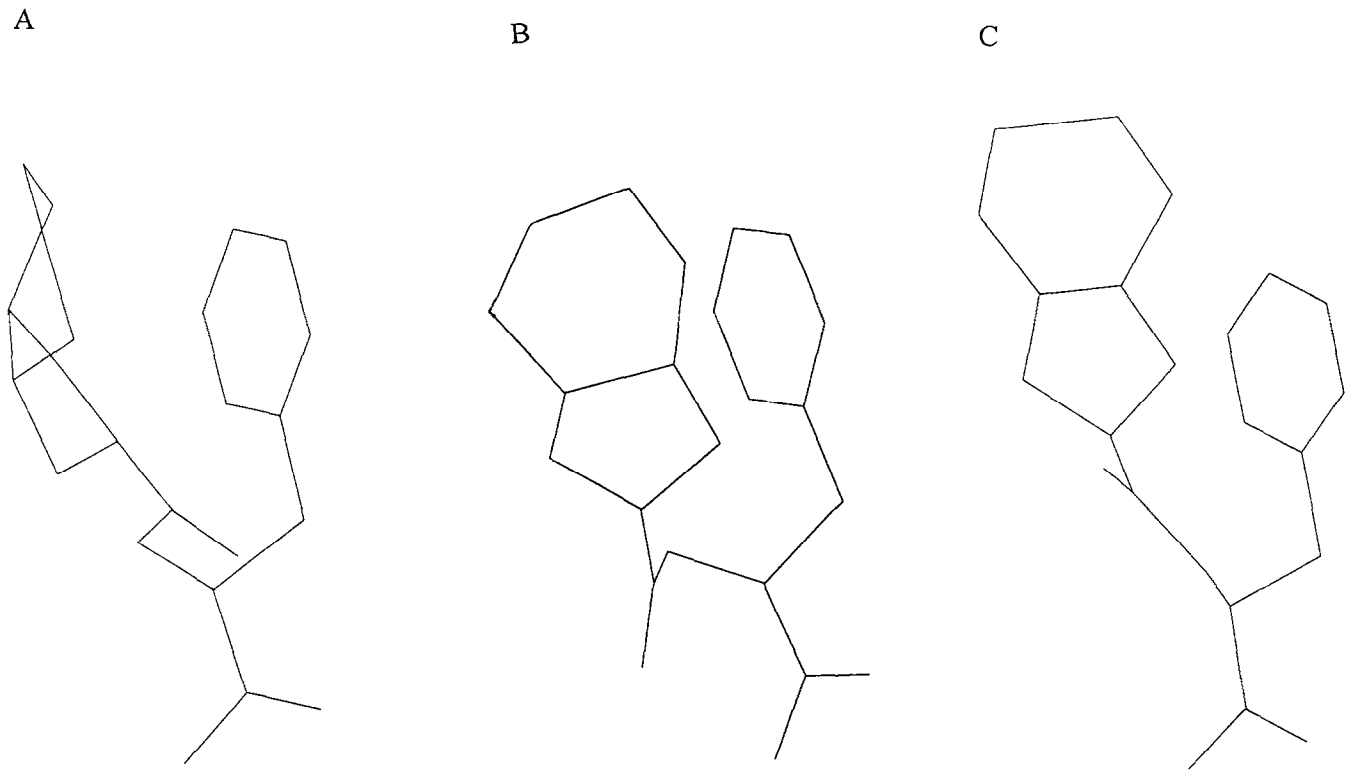

FIG. 9. Skeletal representation of the KADI structures obtained from Method 1 (A), Method 2 (B), and Method 3 (C). The phenyl cycle is represented in the same orientation.

Figures 6 and 7 show the most stable conformations obtained by the different methods for both conformers of KAD (KADI and KADII, respectively). Because no stereospecific assignments were available from the NMR spectra, different calculations were performed to try out the different possible combinations for the assignment of the a/b CH_2 protons. It turned out that this assignment was different for KADI and KADII. The proton–proton distances measured in each of the structures shown in Figs. 6 and 7 are listed in Table 3A (KADI) and 3B (KADII); the proton pairs are labeled as in Fig. 1.

For Methods 1 and 2, a good agreement is observed between the experimental data and the proton–proton distances measured in the modeled structures, but only when restraints are applied. Indeed, most of the values do not exceed 10–15% of the values derived from the NMR spectra. It should be emphasized that Method 1 gives better results, with no violations for the unambiguous NMR distances, whereas Method 2 shows distance discrepancies for the 1a/3b, 6b/7, and 8a/10a proton pairs in KADI and for the 1a/10a and 1b/10b pairs in KADII. Without restraint (on 8b/14 distance in Method 1 and no restraint at all in Method 2), the distance between protons 8b and 14, representative of the interaction between the phenyl cycle and the perhydroisoindole ring, becomes larger, with the cycles no longer interacting (Fig. 8). This decreased interaction is shown by an "open" conformation for the structure obtained with Method 2, both cycles being moved away from each other (Fig. 8, lower panel); however, in the structure yielded by Method 1, the plane of the phenyl cycle is moved by approximately 90°, together with a change on the perhydroisoindole ring conformation (Fig. 8, upper panel), resulting in the disappearance of the interaction between both cycles (the planes of the cycles are almost perpendicular to each other). It is worth noting that an open conformation, similar to that observed for the structure derived from Method 2, is generated for KAD 1229 when the solvation energy term is omitted in Method 3 (data not shown).

The structure obtained with Method 3 (Fig. 6, lower panel), i.e. without any restraint but taking into account the hydrophobic interaction, is also in agreement with the NMR data, especially concerning the 8b–14 distance. However, the distances involving the 10a and 10b protons are in discrepancy with the experimental data, which may be due to the inter-ring chain portion in the neighborhood of the C=O group, which displays a very different conformation from that obtained with the other methods (Fig. 6, upper and middle panels), which are, on the contrary, in good correlation with the NMR data. This different conformation might be due to the fact that the bond lengths and angles are kept constant in Method 3, unlike in Methods 1 and 2 (see below). This difference is also observed in Fig. 9, where the three KADI structures, which best fit the NMR data, are represented with a similar orientation of the phenyl cycle. Moreover, we observed that the interaction be-

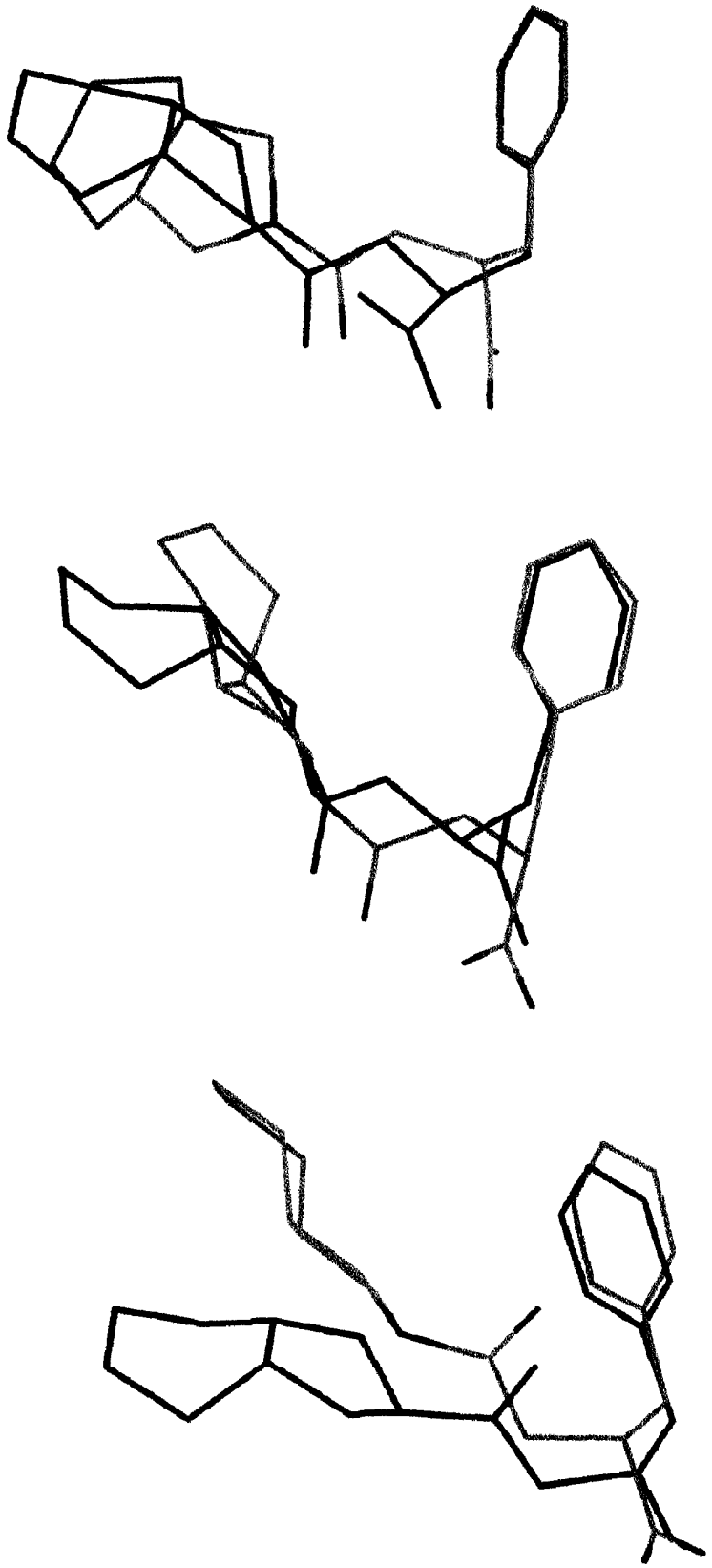

FIG. 10. Superposition of the KADI (in colors as defined in Fig. 6) and KADII (in green) conformations obtained by Methods 1 (upper panel), 2 (middle panel) and 3 (lower panel).

TABLE 4. Population distribution (%) of KADI and KADII based on their relative conformational energy

	KADI	KADII
Method 1	51	49
Method 2	50	50
Method 3	52	48

tween the perhydroisoindole and phenyl rings is stronger in the KADI structures obtained with Methods 2 (Fig. 9B) and 3 (Fig. 9C), their plane being almost parallel to each other, than in the structure generated by Method 1 (Fig. 9A), in which the perhydroisoindole cycle is twisted. It should also be noted that, although the relative position of both cycles is similar in the three structures, the conformation of the chemical groups (called *chain* below) linking these cycles is quite different.

Concerning the difference between KADI and KADII, Fig. 10 shows the fitting between KADI and KADII structures obtained by the three different methods. For the structures generated by Methods 2 and 3, the middle and upper panels of Fig. 10 reveal that the conformational difference is due to a different position of the six-membered ring in the perhydroisoindole moiety with respect to the remaining part of the molecule that is essentially unaffected. For the KADII structure arising from Method 1 (Fig. 10, upper panel), the conformation of the perhydroisoindole ring is twisted as compared with the KADI, rather than displaying the above-mentioned modified six-membered ring; moreover, the conformation of the chain linking both cycles is more elongated in KADII than in KADI. Nevertheless, in all three approaches the conformational changes can be summarized by a different geometry at the level of the six-membered ring of the perhydroisoindole ring, which lies farther away from the aromatic ring in KADII than in KADI.

Table 4 gives the relative probability of KADI and KADII conformations, calculated as described in Material and Methods. It is worth noting that the populations of KADI and KADII, based on their conformational energy, is of the same magnitude, as supported by the presence of equally split intense resonances in the NMR spectra (Fig. 2).

In view of the results, the three molecular modeling approaches can be compared. First, it is obvious that these three modeling methods yield satisfactorily similar structures. However, they are not completely identical, especially at the level of the inter-ring chain. For the structure from Method 3, its conformation might be incorrect (see above); Methods 1 and 2 provide two possible existing conformations, which are in reasonable agreement with the experimental NMR data. Similarly, the twist of the perhydroisoindole ring in the Biosym structure may be an alternative existing conformation, although the other simulations reveal that the hydrophobic interaction between cycles may be energetically very favorable.

Concerning the different force fields used, the MM+ force field was applied in Method 2 [12] and the CVFF in Method 1. Both force fields take into account similar energetic fields, i.e. the distortion of bond lengths and angles, the VdW, electrostatic, and torsional potentials. The VdW contribution is expressed as the Lennard-Jones potential in CVFF; in contrast, the repulsive term is an exponential, with an attractive $1/r^6$ dispersion interaction in MM+. Method 3 is restricted to the torsional potential and the VdW (exponential repulsive term, as in MM+) and electrostatic energies but contains an additional term that includes hydrophobic interactions between atoms by the calculation of a solvation energy, which includes a factor representing the solvent-accessible surface. These equations are empirical but appear to simulate the role of the intramolecular hydrophobic interaction in a satisfactory manner, as revealed by the NMR data in the present report and our earlier studies [14, 15].

The importance of such a force field has been underlined in different examples, such as the experimental replacement of a buried salt bridge in the Arc repressor by interacting hydrophobic residues, the "hydrophobic" mutants being shown to be at least as stable as the wild type [19]. The introduction of solvation energy also permitted us to simulate the folding of small soluble proteins with an accuracy close to that of the experimental determination (r.m.s. ca. 3 Å) [15]. Furthermore, the role of the hydrophobic interaction has recently been highlighted by the conformational study of other molecules of the meglitinide family [4] to which KAD 1229 belongs. These molecules are hypoglycemic drugs that share a common structural feature: they possess a U shape, each "branch" of the U bearing a hydrophobic ring. When the hydrophobic interaction between these cycles decreases, i.e. when the U shape of the molecule is less marked, its biological activity also decreases, as shown for inactive conformers of some of these drugs [4]. Furthermore, this hydrophobic interaction was also observed for active hypoglycemic drugs that were chemically very different from the members of the meglitinide family. It is worth noting that the present NMR results appear to confirm experimentally the presence of such a hydrophobic interaction.

CONCLUSION

Molecular modeling generates structures in agreement with the NMR data in two different cases:

1. External restraints based on the NMR results have to be introduced, as in Methods 1 and 2. However, this approach may present disadvantages. Indeed, the long range distances measured by 2D NOEs (>3–4 Å) are subject to greater uncertainties than shorter distances. Hydrophobic interactions that may occur at even longer distance (>4–5 Å) may become hardly detectable by NMR. As a consequence, if external restraints are used and if hydrophobic interactions between domains of a

molecule involve distances exceeding typically 4 Å, this information may get lost and a less accurate modeled structure may be generated.

2. A term recognizing the hydrophobic interaction is introduced in the force field, thereby allowing an *ab initio* modeling. This situation corresponds to constraints *internal* to the system. Furthermore, in this approach as in the NMR experiments, the structure is dependent of the solvent nature because the solvent is implicitly present in the empirical equation (by the r_{sol} term) defining the solvation energy (see Material and Methods). This method could be refined if the bond length and valence angle distorsion were included. Indeed, the structure obtained by Method 3 yields a good visualization of hydrophobic interaction but presents some violations with the NMR data, such as the distances implying proton 10.

Thus, combining both modeling approaches (i.e. external restraints and hydrophobic interaction) can contribute to improve the statistical significance of NMR long range distances relevant to the molecular structure (using Method 3). These distances result from intramolecular interactions such as hydrophobic ones, which play an essential role in the biological activity of some molecules, as shown for the hypoglycemic drugs of the meglitinide family [4].

The information presented in this report on the two stable conformers of KAD-1229 reinforces the view that the hydrophobic interaction between the phenyl cycle and perhydroisoindole ring of KAD-1229 represents an essential determinant of its molecular conformation [4]. This result is consistent with the proposal that hydrophobic interaction plays a major role in the pharmacological activity of meglitinide analogs and as such may account for both differences in insulinotropic efficiency between distinct analogs and the conformational specificity of the biological response to some of these hypoglycemic agents.

We show here that the equation of the solvation energy not only can serve in determining the three-dimensional structures of small soluble proteins [15] but can also be extended to the study of molecules from other domains of biology and biochemistry, as shown here for hypoglycemic drugs.

P.V. is a senior research assistant at the National Fund for Scientific Research of Belgium (NFWO). This work was supported by the Belgian Nationale Loterij (grant 9.0006.93), the Belgian Fonds voor Kollektief Fundamenteel Onderzoek (grant 2.0094.94), and by the Research Council of the Vrije Universiteit Brussel. L.L. is recipient of a grant Télévie (FNRS); R.B. is Research Director at the National Fund for Scientific Research of Belgium (FNRS). We are grateful to the Association Française de Lutte contre la Mucoviscidose for financial support. This work was also supported by the Fonds de la Recherche Scientifique Médicale (grants 2.4534.95 and 3.4513.94).

References

1. Malaisse WJ, Stimulation of insulin release by non-sulfonylurea hypoglycemic agents: the meglitinide family. *Horm Metab Res* **27:** 263–266, 1995.
2. Malaisse WJ and Sato F, Insulinotropic aciton of (2S)-2-benzyl-3-(*cis*-hexahydro-2-isoindolinylcarbonyl)propionate. I. Secretory and cationic aspects. *Gen Pharmacol* **26:** 1313–1316, 1995.
3. Malaisse WJ, Insulinotropic action of meglitinide analogs: modulation by an activator of ATP-sensitive K^+ channels and high extracellular K^+ concentrations. *Pharmacol Res*, in press.
4. Lins L, Brasseur R and Malaisse WJ, Conformation analysis of non-sulfonylurea hypoglycemic agents of the meglitinide family. *Biochem Pharmacol* **50:** 1879–1884, 1995.
5. Bax A, Griffey RH and Hawkins BL, Correlation of proton and nitrogen-15 chemical shifts by multiple quantum NMR. *J Magn Reson* **55:** 301–315, 1983.
6. Bax A and Summers MF, ^1H and ^{13}C assignments from sensitivity enhanced detection of heteronuclear multiple bond connectivity by 2D multiple quantum NMR. *J Am Chem Soc* **108:** 2093–2094, 1986.
7. Griesinger C, Sørensen OW and Ernst RR, Practical aspects of the E.COSY technique. Measurements of scalar spin-spin coupling constants in peptides. *J Magn Reson* **75:** 474–492, 1987.
8. Macura S and Ernst RR, Elucidation of cross relaxation in liquids by two-dimensional NMR spectroscopy. *Mol Phys* **41:** 95–117, 1980.
9. Marion D and Wüthrich K, Application of phase sensitive two dimensional correlated spectroscopy (COSY) for measurements of ^1H–^1H spin-spin coupling constants in proteins. *Biochim Biophys Res Commun* **113:** 967–974, 1983.
10. Neuhaus D and Williamson MP, *The Nuclear Overhauser Effect in Structural and Conformational Analysis*. VCH, New York, 1989.
11. Andersen NH, Eaton HL and Lai X, Quantitative small molecule NOESY. A practical guide for derivation of cross-relaxation rates and internuclear distances. *Magn Reson Chem* **27:** 515–528, 1989.
12. Allinger NL, Conformational analysis. 130. MM2. A hydrocarbon force field utilizing V1 and V2 torsional terms. *J Am Chem Soc* **99:** 8127–8134, 1977.
13. Brasseur R and Deleers M, Conformational analysis of 6-cis and 6-trans leukotrienes-B4-Ca2+ complexes. *Proc Natl Acad Sci USA* **81:** 3370, 1984.
14. Lins L and Brasseur R, The hydrophobic effect in protein folding. *FASEB J* **9:** 535–540, 1995.
15. Brasseur R, Simulating the folding of small proteins using the local minimum energy and the free solvation energy yields native-like structures. *J Mol Graphics* **13:** 312–322, 1995.
16. Nelder JA and Mead R, A simplex method for function minimization. *Computer J* **7:** 308–313, 1965.
17. Rahman M and Brasseur R, WinMGM: a fast CPK molecular graphics program for analyzing molecular structure. *J Mol Graphics* **12:** 212–218, 1994.
18. Brasseur R (Ed.), TAMMO: Theoretical Analysis of Membrane Molecular Organization. In *Molecular Description of Biological Membranes by Computer-Aided Conformational Analysis*, vol. 1. CRC Press, Boca Raton, 1990.
19. Waldburger CD, Schildbach JF and Sauer RT, Are buried salt bridges important for protein stability and conformational specificity? *Nature Struct Biol* **2:** 122–128, 1995.